Electrochimica Acta 195 (2016) 19–26

Contents lists available at ScienceDirect

Electrochimica Acta

journal homepage: www.elsevier.com/locate/electacta

Dynamic Reference Electrode development for redox potential measurements in fluoride molten salt at high temperature

Gabriela Durán-Klie, Davide Rodrigues, Sylvie Delpech*

Institut de Physique Nucléaire (IPN), Groupe Radiochimie, Université Paris Sud, CNRS, 15 Rue Georges Clemenceau, 91406 Orsay, France

ARTICLE INFO

Article history:
Received 22 November 2015
Received in revised form 6 February 2016
Accepted 8 February 2016
Available online 23 February 2016

Keywords:
molten salt reactor
corrosion

ABSTRACT

Measurement of redox potential in fluoride media is a major problem due to the difficulty to design a reference electrode with high stability, high mechanical resistance and high accuracy. In the frame of molten salt reactor studies, a dynamic reference electrode (DRE) is developed to measure redox potential in fluoride molten salt at high temperature. DRE is based on the *in-situ* generation of a transient redox system. The choice of the redox couple corresponds to the cathodic limit of the molten salt considered. As a preliminary step, the demonstration of feasibility of generating a DRE was done in LiF-NaF-KF (46.5–11.5–42 mol%) media at 500 °C. In this salt, the reference redox system generated by coulometry at applied current is KF/K, metallic potassium being electrodeposited on a tungsten wire electrode. The validation of the DRE response and the experimental optimization parameters for DRE generation were realized by following the NiF_2/Ni redox potential evolution as a function of NiF_2 concentration in the fused salt.

The current value applied for DRE generation was optimized. It depends on the amount of metallic cations contained in the fused salt and which can be electrochemically reduced simultaneously during the DRE generation. The current corresponding to the DRE generation has to be 4 times greater than the current corresponding to the reduction of the other elements.

1. Introduction

The molten salt fast reactor (MSFR) is an innovating concept of the molten salt reactor (MSR) developed by CNRS (France) since 2004 [1–4]. This reactor is a nuclear concept of Generation IV, currently in a developing phase (particularly in the frame of the European project SAMOFAR supported by HORIZON H2020), and derived from other concept described in the reference [5]. This concept is designed for the use of a liquid nuclear fuel composed of a mixture of fluoride salts (liquid in the reactor operation temperature range, 650–850 °C), which circulates from the reactor core to the heat exchangers. This reactor is adapted to work under thorium fuel cycle (Th^{232}-U^{233}). The nuclear fuel retained for the MSFR is constituted of the fluoride salts, LiF-ThF_4-(UF_4-UF_3) (77–19–4 mol%). In this concept, the structural materials corrosion is an issue, because of the reactions involving by contact between materials and fuel salt. Several factors promote the corrosion of these materials, such as oxidizing impurities (O_2, H_2O, F_2), secondary products of chemical reactions (HF) or fission products, as well as the high working temperature. Also, an alteration of the chemical and physical properties of the salt has been reported due to the temperature gradient between hot and cold points in the circulator which causes a variation of the salt chemical composition [6–8]. Currently, the development and evaluation of new materials (essentially Ni-based alloys with low Cr amounts) that are more resistant to operating conditions of the reactor constitutes a large research focus. On the other hand, the development of methods to prevent corrosion is an approach of major interest to avoid the chemical damages. It was demonstrated that the redox potential of the salt is the most influential parameter in the structural materials corrosion process. Therefore the fuel redox potential control can be used for materials oxidation prevention. The redox potential can be controlled using an internal redox "buffer" which fixes the molten salt potential. The redox buffer chosen for MSFR application is constituted of the two soluble oxidation states of uranium, UF_4 and UF_3. In this way, the fuel salt redox potential is given by the Nernst relation:

$$E_{UF_4/UF_3} = E^{\circ}_{UF_4/UF_3} + \frac{2.3RT}{nF} * \log\frac{[UF_4]}{[UF_3]} \quad (1)$$

Where, E is the redox potential of the salt, E° is the apparent standard potential of UF_4/UF_3 (V), R is the ideal gas constant

* Corresponding author.
E-mail address: delpech@ipno.in2p3.fr (S. Delpech).

http://dx.doi.org/10.1016/j.electacta.2016.02.042
0013-4686/

(=8.314 J.K^{-1}.mol^{-1}), T is the temperature (K), n is the number of exchanged electrons, F is the Faraday's constant (=96500 C), $[UF_4]$ and $[UF_3]$ are respectively the concentrations of UF_4 and UF_3 in the fuel salt.

The relation (1) shows that a modification of the $[UF_4]/[UF_3]$ ratio will cause a redox potential variation of the fuel salt. An increase of the salt potential leads to the oxidation of structural materials, particularly oxidation of Cr [6]. The redox potential has to be measured *in-situ* in the reactor core because it was shown that the potential of the fuel salt increases with the operation time because of the fission reaction [6]. The control (and decrease) of the potential can be realized by the addition of given amounts of reductive element, metallic uranium for instance. Then, the chemical reaction (2) will occur in the salt:

$$U + 3UF_4 \rightarrow 4UF_3 \quad (2)$$

Gibilaro et al. [9] have shown by electrochemical techniques a fast kinetic of this reaction in an inactive fluoride salt.

The measurement of the redox potential in the fuel salt requires a reference electrode with high mechanical resistance and high accuracy. The concentration ratio $[UF_4]/[UF_3]$ can vary from 10 to 100 which corresponds to a potential range of 0.2 V. A corrosion study has been realized by the Oak Ridge National Laboratory [10]: metallic samples were introduced in molten salts which composition varies from 10 to 100. At the end of the corrosion tests, the samples were characterized by SEM analysis. It was observed that for a ratio lower than 60, no corrosion is observed. This was observed by SEM characterization of alloys dipped in several compositions of molten salts. The aim of this paper is to present a methodology to prepare an *in-situ* dynamic reference electrode by applying a cathodic current in a molten salt containing metallic cations and to optimize the internal generation conditions. As a preliminary step, tests were done in the inactive fluoride salt LiF-NaF-KF-NiF_2 (0.1–1 mol%) molten salt at 500 °C.

2. State of the art

Various reference electrodes have been developed for their use in molten fluorides [11]. The most serious problems encountered in the development of reference electrodes for fluorides deal with containment and materials of construction. Alumina rod that was wet by the solvent was employed as the salt bridge, but some solubility of alumina in the solvent and the presence of undesired oxide ions were observed [12,13]. Boron nitride (BN), which is normally an insulator in fluoride melt, has been used. It is slowly impregnated by the melt to provide ionic contact [14–16]. In these conditions a compartment of BN is filled with the molten salt containing generally NiF_2 and a Ni wire ensuring the electrical contact. The wetting of BN occurs in about 24 hr in molten LiF-NaF-KF while a longer period is usually required for more acidic media (10–14 days in LiF-BeF_2-ZrF_4 molten salt at 500–550 °C [14]). BN coated graphite was also tested as reference electrode [17]. A reference electrode for molten fluorides employing a single-crystal LaF_3 membrane for separation was also described and used for electrochemical determinations [18–20]. Generally the redox system considered for the reference electrode is Ni(II)/Ni because it is a reversible system in fluoride solvents [14]. However, prolonged contact with fluoride melts will eventually deteriorate the BN because of a chemical reaction between NiF_2 and BN [11]. The redox system AgCl/Ag has also been employed in the BN container [16] but this redox system cannot be used at temperatures higher than 960 °C due to silver fusion. In this case, the molten salt introduced in the BN container is a chloride media, AgCl/Ag being a reversible system in these conditions. Pizzini [21] used a BN compartment containing a platinized platinum foil. A stable potential is observed after 10 mn of hydrogen bubbling.

Another type of references is based on the generation of an internal reference electrode. This option was retained for the MSFR application. Indeed, the reference electrode being immerged in the reactor core, it requires a high mechanical resistance which is not reached by the use of BN containment. The reference electrode has to be made of a metallic rod, chemically inert, stable at high temperatures, sensitive to the change of medium composition, with a high corrosion resistance and high mechanical resistance. Moreover, the reference redox system has to be reversible. Previous works present the *in-situ* electrochemical generation of a reversible redox system by an anodic [22] or cathodic reaction [23–25]. Ema et al. [23] have developed a dynamic reference electrode of Li, $K/Li^+,K^+$ for the electrochemistry in LiF-KF eutectic melt. This electrode is obtained by a constant current applied on a nickel rod. A Li-K alloy is deposited in a molar fraction of 2:1. The equilibrium potential of the alloy immerged in the fluoride salt is in agreement with thermodynamical calculations and measurements of HF/H_2 gas electrode. Stability and reproducibility have been obtained for the measurements. Adhoum et al. [22] have studied the Na^+/Na, Ni^{2+}/Ni, Mo^{3+}/Mo and the Fe^{2+}/Fe redox systems for a future use as dynamic reference electrode in the molten sodium fluoride at 1025 °C. The electrochemical study through convolution voltammetry shows the reversibility of Fe^{2+}/Fe system. The small dispersion of the measurements allows this system to be used as a dynamic reference electrode. More recently, Afonichkin et al. [24], have developed a device for redox potential measurements (DRPM) in LiF-NaF-BeF_2 (15-58-27) mol% molten salt at 600 °C. The DRPM is based on a system with three electrodes and two of them are used for the dynamic reference electrode generation. The dynamic reference electrode is made of a tungsten electrode covered by metallic Be, the reference redox system being Be(II)/Be. An accuracy of ±5 mV is obtained for this dynamic reference electrode. The performance of DRMP has been tested in a loop under thermal convection during 1200 h. The on-line tests showed the stability and reliability of the device. Qiao et al. [25] have developed an internal reference electrode by electrochemical formation of Au_2Na alloy in FLiNaK molten salt.

3. Technical

LiF, NaF, KF, NiF_2 are provided by Sigma Aldrich (>99% purity) W, Ni are provided by Goodfellow (>99.9% purity). Graphite is provided by Carbon Lorraine (>98% purity).

The molten salt is a mixture of LiF-NaF-KF (46.5–11.5–42) mol% known as FLiNaK. The FLiNaK mixture is introduced and mixed in a glassy carbon crucible (HTW Hochtemperatur-Werkstoffe GmbH) disposed in a cell. The cell is made of Pyrex and constituted of two parts (top and bottom). The air tightness is maintained using a locking screw. The electrochemical cell is then introduced in a tubular furnace (80 cm diameter) connected to a regulation monitor provided by THERMOLAB/Spain. Electrochemical measurements are performed with a potentiostat-galvanostat model PAR 263A coupled with a PC computer.

The purification of the salt is performed by keeping the cell under vacuum for 24 h at 573 K. next, the mixture is melted by increasing the temperature to 773 K. All the experiments are performed under argon gas (Air Liquide) flow at 773 K. NiF_2 is added in the molten salt at various concentrations ranging between 0.1 and 1 mol%.

The working electrodes are prepared using a Ni wire (1 mm diameter) and a W wire (1 mm diameter). The auxiliary electrode used for DRE generation is a graphite rod (3 mm diameter, Carbon

Lorraine). The tightness of the top of the cell is ensuring by introducing electrodes through SVL caps.

The impedance spectroscopy measurements have been performed using a potentiostat PARSTAT 4000. These determinations concern only the electrolyte resistance. Therefore only the frequency range corresponding to the high frequencies were studied (from 10^5 to 200 Hz). The working electrode used was made of a gold wire (S = 0.39 cm^2), the reference electrode was a quasi-reference made of platinum wire and the counter electrode a tungsten wire. The impedance diagrams were recorded at the open circuit potential. The fit of the diagrams has been done using Kaleidagraph version 4.0 and a lab-made special macro.

4. Results and discussion

The objective of our work is to develop a dynamic reference electrode by internal generation in the fluoride molten salt LiF-ThF_4-UF_4. If the reference dynamic electrode is prepared by applying a cathodic current in order to cover an inert electrode with metallic thorium and then, fix the redox system Th(IV)/Th as the reference electrode potential, the deposit will be polluted with metallic uranium and, in the case of the nuclear fuel with all the reducible elements contained in the fuel salt.

4.1. Choice of the reference electrochemical system in FLiNaK molten salt

The aim of this paper is to present a methodology to prepare a dynamic reference electrode by applying a cathodic current in a molten salt containing metallic cations and to optimize the internal generation conditions. As a preliminary step, tests were done in the inactive fluoride salt LiF-NaF-KF-NiF_2 (0.1–1 mol%) molten salt at 500 °C. In this salt, the potential of the dynamic reference electrode obtained by the *in situ* generation corresponds to the redox system K^+/K(εNi) on tungsten electrode. Indeed, thermodynamical calculations show that in FLiNaK, KF is the first element of the solvent to be decomposed (Table 1). That was experimentally confirmed by the results reported by Qiao et al. [24]. In the same way, the cathodic limit of LiF-ThF_4-UF_4 (4 mol%) corresponds to the reduction of ThF_4 (Table 1) as it was observed by Rodrigues [26].

Table 1
Decomposition tension of the reactions in FLiNaK-NiF_2 (500 °C) and LiF-ThF_4-UF_4 (650 °C) *(for thermodynamical calculations (HSC database), activity is considered equal to mole fraction).* UF_4 and NiF_2 are solutes.

Reaction	x(MF) *LiF-NaF-KF-NiF_2*	x(MF) *LiF-ThF_4-UF_4*	ΔE (V)/(F_2/F^-)
$LiF \rightarrow Li + 1/2F_2$ (g)	0.46		−5.67
$LiF \rightarrow Li + 1/2F_2$ (g)		0.77	−5.49
$NaF \rightarrow Na + 1/2F_2$ (g)	0.114		−5.27
$KF \rightarrow K + 1/2F_2$ (g)	0.416		−5.13
$ThF_4 \rightarrow Th + 2F_2$ (g)		0.19	−4.75
$UF_4 \rightarrow U + 2F_2$ (g)		0.04	-4.34
$NiF_2 \rightarrow Ni + F_2$ (g)	0.01		-2.93

The voltammograms given Fig. 1 show the reversibility of the systems KF/K and ThF_4/Th which confirms the potentiality of using these systems as reference electrodes (the reference used to record these voltammograms was made of a quasi-reference electrode of Pt).

This paper presents the optimization of the experimental parameters of DRE generation in fluoride media and its validation by following the evolution of a given redox system potential, NiF_2/Ni as a function of NiF_2 concentrations in the salt, the Nernstian behavior of nickel being evidenced by Jenkins et al. [14].

4.2. Reference dynamic electrode preparation for redox potential measurements of NiF_2/Ni in FLiNaK molten salt

The protocol used for the preparation of the dynamic reference electrode consists in applying a cathodic current pulse of 5 seconds through two electrodes, a tungsten electrode (cathode) and a graphite electrode (anode). A tungsten electrode is chosen to support the redox reference system because, based on thermodynamic considerations, this metal is stable in the molten salt used for the molten salt reactor [6] and cannot be oxidized in the redox conditions imposed by the salt. The reference electrode connected

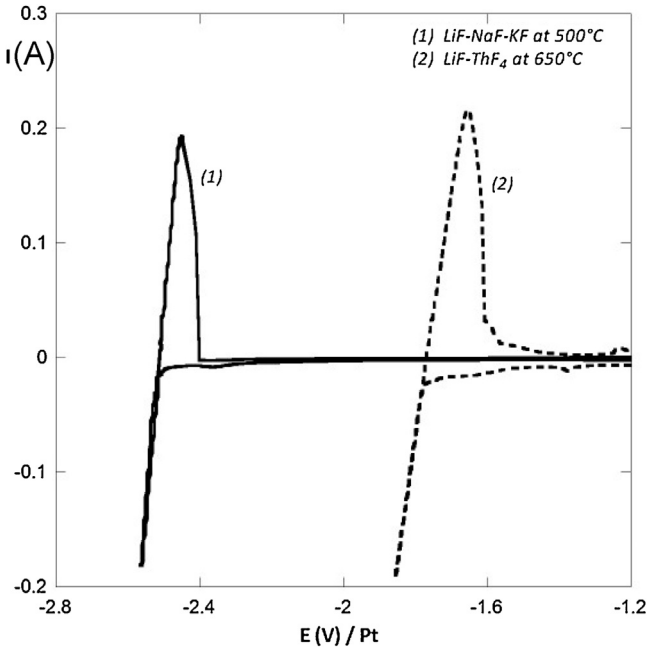

Fig. 1. Cyclic voltammogams in the domain of cathodic limits recorded in FLiNaK at 773 K and LiF-ThF_4 at 923 K on a tungsten working electrode at 100 mV/s against a quasi-reference of platinum.

to the potentiostat is the nickel wire electrode. During the current pulse, metallic potassium is produced and deposited at the surface of the tungsten electrode. At this time, the redox potential of the tungsten electrode is fixed by KF/K redox system. Because the current pulse is very short, the deposit is rapidly oxidized and the potential varies from KF/K redox system to the open circuit potential of the salt. Simultaneously, DRE potential is measured against the nickel wire immersed in the molten salt containing given concentrations of NiF_2.

The determination of the NiF_2/Ni potential against DRE is done by taking the opposite of the potential value given by the potentiostat and corresponding to DRE against Ni.

When the molten salt composition is modified by addition of NiF_2, the first step in the electrochemical process when the cathodic current is applied is the Ni(II) reduction to Ni metal. Then, during the cathodic current pulse, a part of the current is used for the Ni(II) cations reduction process.

For 0.1 mol% of NiF_2 added in FLiNaK molten salt, several pulse current intensities have been applied to generate the DRE. Chronopotentiograms recorded on the tungsten electrode during the electrogeneration of DRE are given Fig. 2. It shows that the redox potential evolution of nickel depends on the intensity of the current pulse applied. That is due to the formation of a co-deposition of nickel and potassium. This co-deposition leads to a mixed potential value ranged between NiF_2/Ni and KF/K redox systems. When the cathodic current is large enough, the redox potential of the DRE tends to a constant and stable value. That indicates that the metallic deposition is mainly constituted of potassium and the potential is not influenced by the small quantities of nickel simultaneously reduced. Otherwise, if a small pulse current magnitude is applied, no reduction of K^+ ions occurs on the electrode surface.

Dynamic reference electrode allows measuring the OCP for a short time which depends on two parameters of the generation process: the electrodeposition time and the intensity of the electrical current applied. In the present work, a pulse of current of 5 s has been chosen as an optimal time condition. This temporal condition guarantees that the thin metallic layer is sufficiently stable for OCP measurements of the system with high reliability and good accuracy. Otherwise, this time is short enough to prevent the modification of the salt composition and/or the formation of high pollution on the anodic side of the electrolysis (on the graphite anode). To limit the influence of the metallic elements co-deposited during the current pulse, the only parameter for DRE generation is the intensity of the current pulse applied.

The open circuit potential evolution of the nickel working electrode recorded against DRE generated by applying a current of −0.3 A during 5 s is shown Fig. 3. Four zones illustrate the potential evolution before, during and after the current pulse:

Zone I, OCP of nickel wire is recorded against tungsten wire before applying the current pulse. Zone II, a cathodic current is applied at the tungsten working electrode. The redox potential of nickel becomes more positive, the K^+ ions reduction to K metallic takes place and a potassium thin layer is formed on the tungsten surface electrode. During this time, DRE is generated. Zone III, the redox potential decreases once the current pulse is achieved. The redox potential measured corresponds to the redox equilibrium potential of K^+/K system. This response remains constant during a time which depends on the passed charge, then both on the current intensity applied and the time pulse. Zone IV, the redox potential of nickel measured against DRE decreases to return to its initial value. This response is characteristic of the oxidation process of the potassium thin layer deposited on the tungsten surface electrode.

The potential difference measured between the zones II and III can be attributed to a quasi-reversible or irreversible charge transfer kinetic or in the case of a reversible system that can correspond to an ohmic drop. The voltamograms recorded in FLiNaK in the cathodic side indicates a reversible system for potassium reduction (Fig. 1). To confirm that the potential difference is due to ohmic drop, the electrolyte resistance has been determined by impedance spectroscopy (Fig. 4) using a same approach already described [27]. This kind of measurement does not require recording an impedance diagram in a large frequency range. It is the reason why the impedance diagram was recorded from 10^5 Hz to 200 Hz. The diagram was recorded at the open circuit potential using a gold working electrode in a pure solvent. In these conditions, the faradaic impedance tends to an infinite value because no charge transfer involves. The equivalent electrical circuit chosen to fit the impedance diagram is given Fig. 4. It presents the electrolyte resistance in series with a $R_{ec}//L_{ec}$ circuit which is attributed to the inductance and resistance of the electrical components of the experimental device (this impedance

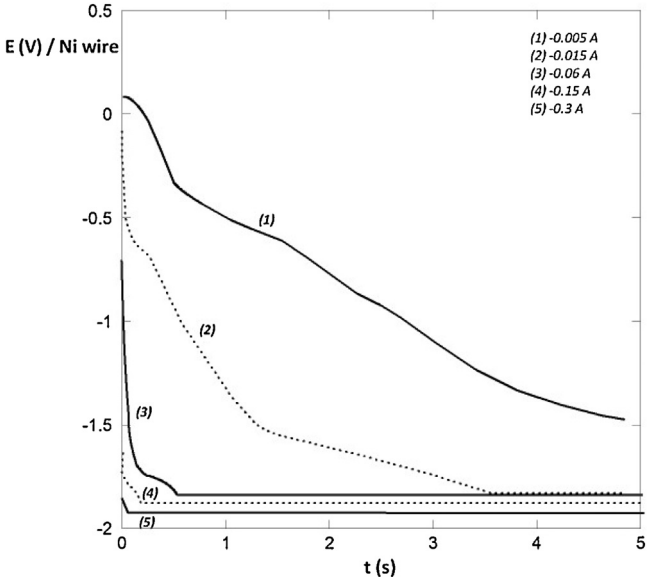

Fig. 2. Chronopotentiograms recorded during DRE generation on tungsten electrode against Ni wire for various applied current in FLiNaK containing 0.1 mol% of NiF_2 at 773 K.

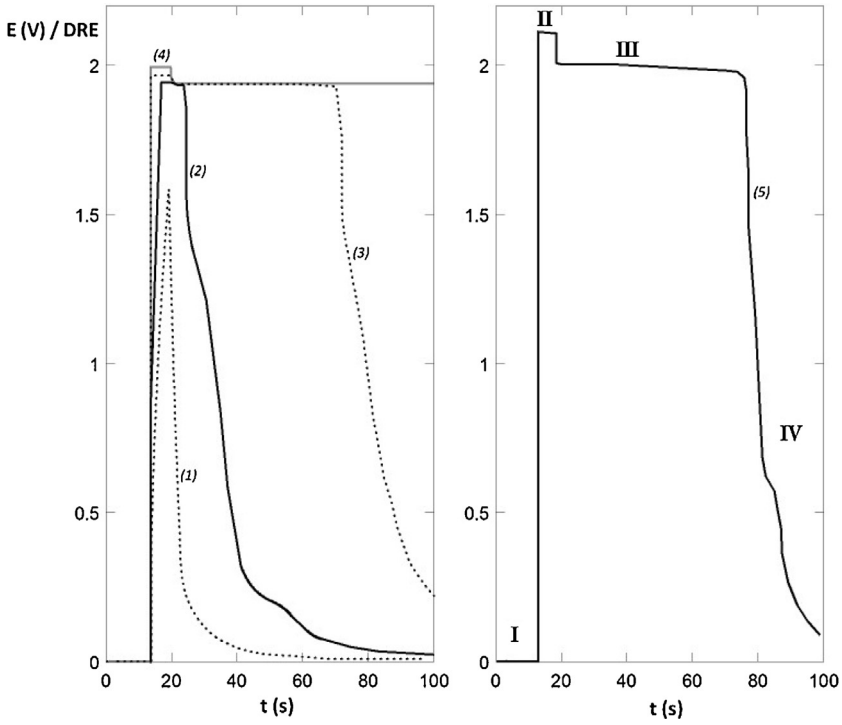

Fig. 3. Chronopotentiograms giving the variation of nickel wire potential against DRE before, during and after DRE generation for various applied current (1) −0.005 A, (2) −0.015 A, (3) −0.06 A, (4) −0.15 A and (5) −0.3 A.

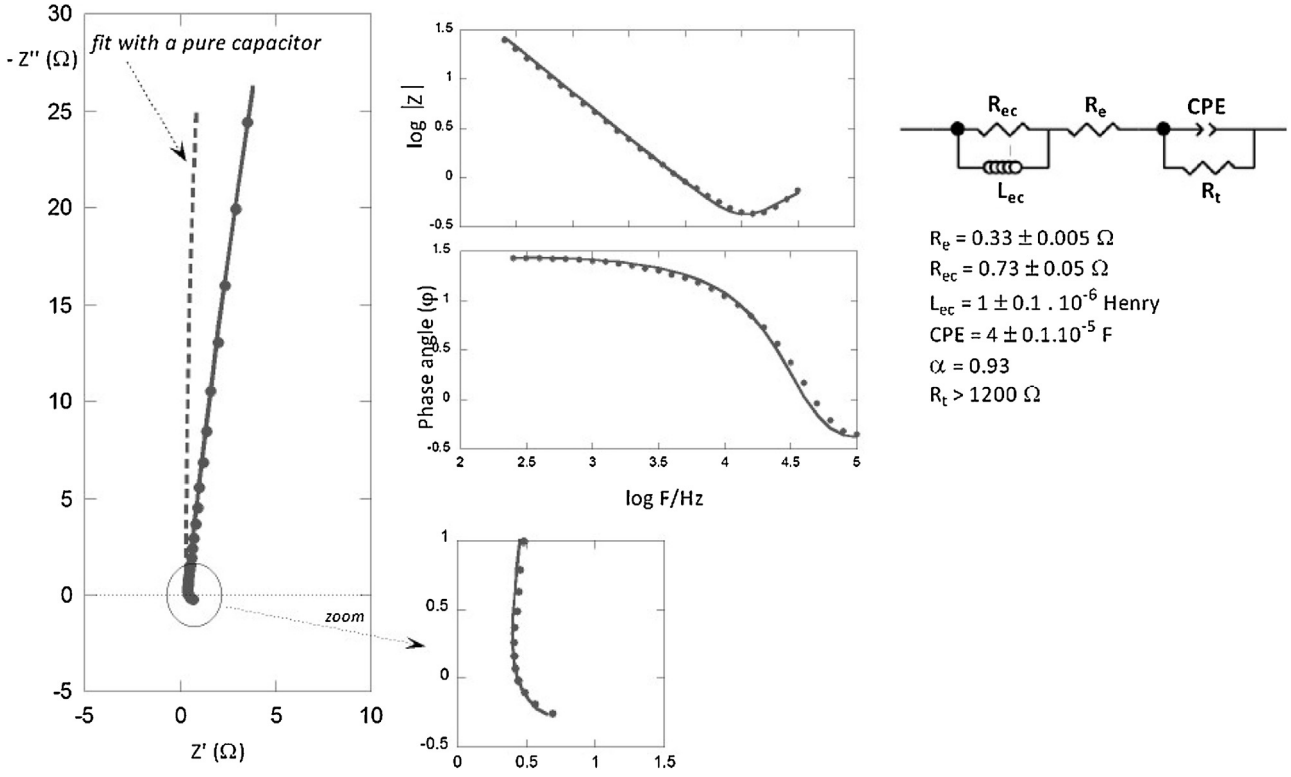

Fig. 4. Experimental (points) and calculated (solid line) impedance diagrams (in Nyquist and Bode representations) realized at Open Circuit Potential in FLiNaK at 773 K on gold working electrode (S = 0.39 cm^2) the equivalent electrical circuit and the input data used for the fit. Broken line: calculation of the impedance with a pure capacitor.

is observed only for impedances lower than 1 Ω), in series with a CPE which is the Constant Phase Element usually used to describe the roughness of solid metal electrodes [28], the CPE being in parallel with the faradaic impedance which is considered here equal to a resistance. The constant phase element is used preferentially to a pure capacitor to obtain a more accurate fit of the diagrams. Indeed, a pure capacitor, as it is shown in Fig. 4 (broken line in the Nyquist plot), is not able to fit the small deviation frequently observed in electrochemical impedance spectra. R_e is the electrolyte resistance and R_t the charge transfer resistance. The value of R_t cannot be determined, we can only give a lower limit value (1200 Ω). An electrolyte resistance of 0.33 Ω has been measured at high frequencies, corresponding to 0.13 Ω.cm^2. The ohmic drop depends on the applied current. Fig. 3 shows that the potential difference between the zones II and III depends on the intensity of the applied current. The ohmic drop has been calculated for the different applied current values and compared with the experimental potential differences measured Fig. 3. The calculated and experimental results are given in Table 2.

These results show the influence of the ohmic drop. That confirms the reversibility of the redox system and it shows that a better accuracy is reached by measuring the potential in the zone III of Fig. 3, because this value is never depending on the applied current intensity.

4.3. DRE current applied optimization

As explained before, the total current applied is the sum of two contributions, reduction of NiF_2 and reduction of KF. We can write the following relations:

$$I_T = I_K + I_{Ni} \quad (3)$$

where I_T is the total current, I_K and I_{Ni} the currents corresponding respectively to the reduction of KF and NiF_2.

k is defined as:

$$k = \frac{I_K}{I_{Ni}} = \frac{I_T - I_{Ni}}{I_{Ni}} \quad (4)$$

Table 2
Comparison of the ohmic drop and the potential difference experimentally measured between zones II and III as a function of the applied current (R_e = 0.13 Ω. cm^2).

I applied (S = 0.32 cm^2)	ΔE = R*I (V)	ΔE experimental (V)
0.015	0.006	0.007
0.06	0.024	0.024
0.15	0.061	0.060
0.3	0.122	0.122

$$I_T = (k+1) * I_{Ni} \quad (5)$$

To optimize the applied current value necessary to generate the DRE in presence of other metallic reducible cations, the response of DRE was measured for several values of k. The current corresponding to nickel reduction is equal to the cathodic limiting current. To control the k parameter as a function of I_T, the value of I_{Ni} was determined for several concentrations of NiF_2 from steady-state i-E curves established from chronoamperogram samplings (Fig. 5).

For several concentrations of NiF_2 (and then for several values of I_{Ni}), DRE was generated by applying pulse current with various intensities corresponding to several k values as it is described in Table 3. For each experiment, the Ni wire potential was measured against DRE in Zone III. From this measurement we calculate the apparent standard potential of nickel by applying the following relation:

$$E^{\circ *}_{Ni} = E_{exp/DRE} - \frac{2.3RT}{2F} \log x\,(NiF_2) \quad (6)$$

The $E^{\circ *}_{Ni}$ values are reported Fig. 6 as a function of k ratio. This figure shows that for k ratios lower than 4, the generation of DRE is not achieved and the potential measured is wrong. When the DRE generation is done in optimized conditions, the value of $E^{\circ *}_{Ni}$ is a constant equal to 2.17 V/DRE.

The optimization of the experimental conditions to generate a stable and accurate DRE requires the knowledge of the cathodic current used for the reduction of the other metallic cations noted I_{MC}. Then it is possible to estimate the total current required to

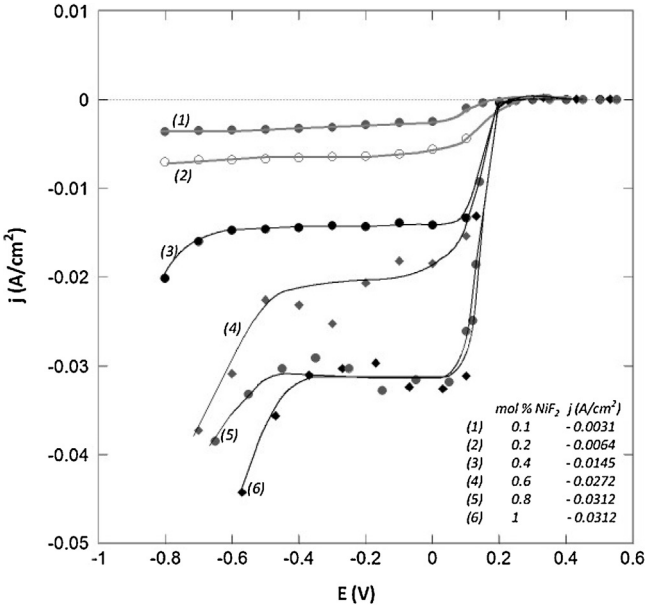

Fig. 5. Steady-state i-E curves determined from chronoamperogram samplings in FLiNaK at 773 K containing various amounts of NiF_2.

Table 3
Variation of the I_K/I_{Ni} ratio with the concentration of NiF_2 in LiF–NaF–KF (46.5–11.5–42) mol% for the different currents applied on a W working electrode.

% mol NiF_2												
0.1		0.2		0.4		0.6		0.8		1.0		
I_{Ni} (A)												
−0.0015		−0.0029		−0.0062		−0.0115		−0.0132		−0.0132		
I/A	*k*	I/A	*k*	I/A	*k*	I/A	*k*	I/A	*k*	I/A	*k*	
−0.005	2.4	−0.008	2.4	−0.015	1.9	−0.06	4.6	−0.06	3.9	−0.3	23.5	
−0.015	9.3	−0.015	5.0	−0.06	10.4	−0.15	13.1	−0.15	11.2			
−0.06	40.1	−0.06	25.9	−0.15	27.6	−0.3	27.0	−0.3	23.5			
−0.15	102.0	−0.15	64.6	−0.3	56.0							
−0.3	204.3	−0.3	128.4									

generate the DRE considering that the intensity of the pulse current has to be equal at least to 4^*I_{MC}.

4.4. DRE validation

Finally, DRE was validated by measuring the potential of a nickel wire against DRE in FLiNaK containing various NiF_2 concentrations. DRE generation was done by applying during 5 seconds a current intensity of −0.3A which corresponds to a *k* parameter higher than 4 in the concentration range of NiF_2 studied. The results obtained are given Fig. 7. The measurement of the potential was realized both in zones II and III. The potential difference measured corresponds to the ohmic drop of 0.122 V previously calculated (Table 2). The best accuracy observed on the measurements realized in the zone III confirms the protocol proposed. The variation of the nickel wire potential with the logarithm of NiF_2 concentration is linear and in agreement with Nernst relation:

$$E_{NiF_2/Ni} = E^{\circ *}_{NiF_2/Ni} + \frac{2.3RT}{2F} * \log [NiF_2] \quad (6)$$

The experimental slope corresponds to the theoretical Nernst slope of 0.077 V at 500 °C which validates the DRE response. The apparent standard potential determined by linear regression is equal to 2.169 V/DRE which is equivalent to the value previously determined.

5. Conclusion

A protocol to generate a dynamic reference electrode has been studied. Its performance was evidenced through the measurement of the NiF_2/Ni redox potential in FLiNaK molten salt. The reference dynamic electrode is based on the formation of a potassium thin layer electrodeposited on a tungsten working electrode by K^+ ions reduction, the reference redox potential being given by the redox system KF/K. Considering that other reducible metallic cations can be present in the molten salt and can be reduced simultaneously as K^+, the applied current has to be high enough to produce a metallic layer made up mainly metallic potassium. The determination of the cathodic limiting current of all the other metallic cations is required before optimizing the DRE generation conditions. Then it was shown that a total current has to be equal at least to 4 times the limiting cathodic current of the other cations.

After DRE generation, the reference electrode can be used. The measurement of the potential has to be performed during the relaxation time as not to be affected by the ohmic drop.

Considering all the conditions of DRE generation and measurements, the validation of DRE was done by measuring the variation of nickel wire potential as a function of NiF_2 concentration in FLiNaK. The agreement between experimental and theoretical

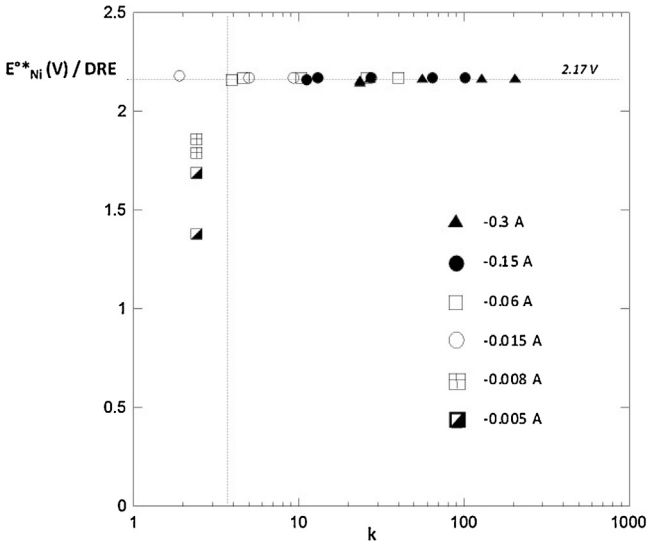

Fig. 6. Variation of the nickel wire potential measured at OCP against DRE as a function of *k* parameter depending on the applied generation current.

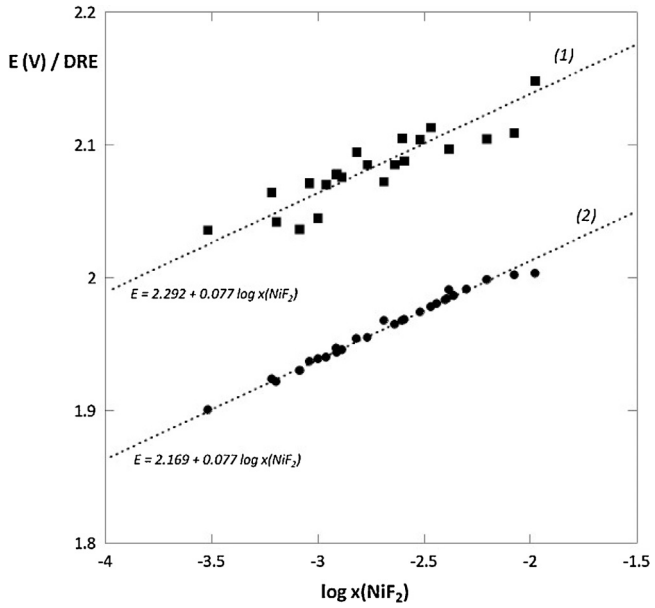

Fig. 7. Variation of the nickel wire potential measured against DRE generated by applying a current of −0.3 A during 5 s, as a function of the logarithm of NiF_2 mole fraction in FLiNaK at 773 K. (1) measurements in zone II (2) measurements in zone III.

variations shows the accurate response of DRE and validates the generation protocol.

In order to evaluate if a deterioration of the tungsten electrode occurs with time, microscopic analysis of the tungsten wire will be done as a function of the number of cathodic pulses applied.

A similar device is currently being studied in the molten salt LiF-ThF_4-UF_4-UF_3 at 650 °C which is the molten salt retained for molten salt fast reactor.

Acknowledgements

The research leading to these results has received funding from the European Community's Seventh Framework Programme under grant agreement n°249696 EVOL, from the French program NEEDS, from CAMPUS-FRANCE and FUNDAYACUCHO for the grant and SOLVAY industry for CIFRE grant.

References

[1] S. Delpech, E. Merle-Lucotte, D. Heuer, M. Allibert, V. Ghetta, C. Le-Brun, J. of Fluorine Chem 130 (2009) 11.
[2] D. Heuer, E. Merle-Lucotte, M. Allibert, M. Brovchenko, V. Ghetta, P. Rubiolo, Annals of Nuclear Energy 64 (2014) 421.
[3] J. Serp, M. Allibert, O. Beneš, S. Delpech, O. Feynberg, V. Ghetta, D. Heuer, D. Holcomb, V. Ignatiev, J. Lean Kloosterman, L. Luzzi, E. Merle-Lucotte, J. Uhlí, R. Yoshioka, D. Zhimin, Progress in Nuclear Energy. 77 (2014) 308.
[4] J. Bouchter, Ph. Dufour, J. Guidez, N. Simon, C. Renault, RGN 2 (2014) 37.
[5] S. Delpech, Molten Salts: fundamental and applications, Elsevier, 2013 (Chapter 24).
[6] S. Delpech, C. Cabet, C. Slim, G. Picard, Materials Today 13 (2010) 34.
[7] G. Santarini, J of Nuclear Materials 99 (1981) 269.
[8] S. Delpech, E. Merle-Lucotte, T. Auger, X. Doligez, D. Heuer, G. Picard, GIF Symposium, (Paris) France, 2009.
[9] M. Gibilaro, L. Massot, P. Chamelot, Electrochimica Acta 160 (2015) 209.
[10] J.R. Reiser, report ORNL/TM-6002, 1977.
[11] D.G. Lovering, R.J. Gale, Molten Salt techniques, Volume 3, Plenum Press, New York, 1987.
[12] K. Grjotheim, Z. Physik, Chem. N.F 11 (1957) 150.
[13] S. Senderoff, G.W. Mellors, W.J. Reinhart, J. Electrochem. Soc. 112 (1965) 840.
[14] H.W. Jenkins, G. Mamantov, J. Electroanal. Chem. 19 (1968) 385.
[15] H.W. Jenkins, G. Mamantov, D.L. Manning, J.P. Young, J. Electrochem. Soc. 116 (1969) 1712.
[16] R. Winand, Electrochim. Acta 17 (1972) 251.
[17] C.G. Kontoyannis, Electrochim. Acta 40 (1995) 2547.
[18] H.R. Bronstein, D.L. Manning, J. Electrochem. Soc 119 (1972) 125.
[19] F.R. Clayton, G. Mamantov, D.L. Manning, J. Electrochem. Soc. 120 (1973) 1193.
[20] F.R. Clayton, G. Mamantov, D.L. Manning, J. Electrochem. Soc. 121 (1974) 86.
[21] S. Pizzini, R. Morlotti, Electrochim. Acta 10 (1965) 1033.
[22] N. Adhoum, J. Bouteillon, D. Dumas, J.C. Poignet, J. Electroanal. Chem. 391 (1995) 63.
[23] K. Ema, Y. Ito, T. Takenaka, J. Oishi, Electrochimica Acta 32 (1987) 1537.
[24] V. Afonichkin, A. Bovet, V. Ignatiev, A. Panov, V. Subbotin, A. Surenkov, A. Toropov, A. Zherebtsov, J. of Fluorine Chem. 130 (2009) 83.
[25] H. Qiao, T. Nohira, Y. Ito, Electrochim. Acta 47 (2002) 4543.
[26] D. Rodrigues, Thesis, University Paris Saclay, 2015.
[27] S. Delpech, D. Rodrigues, S. Jaskierowicz, Electrochimica Acta 144 (2014) 383.
[28] U. Rammelt, G. Reinhard, Electrochim. Acta 35 (1989) 1045.